1   Original article

2   Climate as a driver of adaptive variations in ecological strategies in

3   *Arabidopsis thaliana*

4   François Vasseur[1,2]*, Kevin Sartori[1], Etienne Baron[1], Florian Fort[1], Elena Kazakou[1], Jules

5   Segrestin[1], Eric Garnier[1], Denis Vile[2] and Cyrille Violle[1]

6   **Running title:** CSR variation in a widely distributed species

7   **Affiliation**:

8   [1] CEFE, Montpellier SupAgro, CNRS, Université de Montpellier, Université Paul Valéry

9   Montpellier, EPHE, Montpellier, France

10   [2] Laboratoire d'Ecophysiologie des Plantes sous Stress Environnementaux (LEPSE), INRA,

11   Montpellier SupAgro, UMR759, F-34000 Montpellier, France

12   ***Corresponding author:**

13   François Vasseur: franc.vasseur@gmail.com

14 **Abstract**

15 *Background and aims*. The 'CSR classification' categorizes plant species between stress-tolerators

16 (S), ruderals (R) and competitors (C). Initially proposed as a general framework to describe

17 ecological strategies at the interspecific level, this scheme has recently been used to investigate the

18 variation of strategies within species. For instance, ample variation along the S-R axis was found in

19 *Arabidopsis thaliana*, with stress-tolerator accessions predominating in hot and dry regions.

20 *Methods*. In this study, the range of CSR strategies within *A. thaliana* was evaluated across 426

21 accessions originating from North Africa to Scandinavia. A position in the CSR strategy space was

22 allocated for every accession based on three functional traits: leaf area, leaf dry matter content

23 (LDMC) and specific leaf area (SLA). Results were related to climate at origin and compared to a

24 previous study performed on the same species. Furthermore, the role of natural selection in

25 phenotypic differentiation between lineages was investigated with Q_{st}-F_{st} comparisons, using the

26 large genetic information available for this species.

27 *Key results*. Substantial variation in ecological strategies along the S-R axis was found in *A.*

28 *thaliana*. By contrast with previous findings, stress-tolerator accessions predominated in cold

29 climates, notably Scandinavia, where late flowering was associated with traits related to resource

30 conservation such as high LDMC and low SLA. Because of trait plasticity, variations in CSR

31 classification to growth conditions were also observed for the same genotypes.

32 *Conclusions*. There is a latitudinal gradient of ecological strategies in *A. thaliana* as a result of

33 within-species adaptation to climate. Our study also underlines the importance of growth conditions

34 and of the methodology used for trait measurement, notably age versus stage measurement, to infer

35 the strength and direction of trait-environment relationships. Taken together, this highlights the

36 potential and limitations of the CSR classification to explain functional adaptation to the

37 environment.

38 **Key words**: *Arabidopsis thaliana*, adaptive differentiation, climate, CSR classification, ecological

39 strategy, functional trait, genetic diversity, Grime triangle, latitudinal gradient, Q_{st}-F_{st}, trait-

40 environment relationships.

Introduction

Screening approaches allow species comparison on the basis of key 'functional traits', *i.e.* traits representative of major functions such as growth, stress resistance, defence and reproduction (Keddy 1992, Violle *et al.* 2007). Trait-based approaches in plant ecology have a long history of classifying plant species into functional groups according to the combination of phenotypic traits they exhibit (Garnier *et al.* 2016). Such approaches have been mainly applied for comparative analyses at the interspecific level to identify general patterns of trait variation and covariation. However, recent comparative analyses argue for a better integration of intraspecific variability for understanding the role of trait covariation in plant adaptation, ecosystem functioning and community assembly (Albert *et al.* 2010, 2011; Violle *et al.* 2012; Siefert *et al.* 2015).

Amongst the prominent examples of plant species classification, Grime (1977) defined ecological strategies based on the idea that there are two main ecological drivers of plant diversification: (i) the effect of stress related to the shortage of resources (*e.g.*, nutrient, water and light), and (ii) the effect of disturbance. Stress is viewed in this context as any environmental factors or combination of factors that reduce plant growth, although the shortage of nutrients, water or light can each affect specific traits (Grime and Hunt, 1975; Grime 1977; Hodgson *et al*. 1999). By contrast, disturbance is viewed as factors that cause the partial or total destruction of plant biomass, which include grazing, trampling, mowing, but also extreme climatic events such as severe drought, frost and fire (Grime and Hunt, 1975). Differences in disturbance and stress intensity are expected to result in quantitative variation in three ecological strategies: (i) stress-tolerators (S) in stressed, resource-poor habitats with low disturbance, which invest resources to protect tissue from stress damages, (ii) ruderals (R) in resource-rich environments associated with repeated disturbance, which invest resources into rapid reproduction and propagule dispersal, and (iii) competitors (C) in highly productive habitats with low stress intensity and disturbance, which invest resources into the rapid growth of large organs to outcompete neighbours. The S-R axis is traditionally viewed as an axis of resource-use variations at the leaf level (Pierce *et al.* 2013), where ruderality is associated

3

67   with acquisitive resource-use (characterized by short-lived, flimsy leaves with high nutrient

68   concentration and high net photosynthetic rate), and stress-tolerance is associated with conservative

69   resource-use (characterized by long-lived, tough leaves with low nutrient concentration and low net

70   photosynthetic rate). By contrast, variation of competitive ability along the C axis is thought to

71   reflect variation in plant and organ size, and it is expected to operate where the impacts of stress and

72   disturbance are low (Grime 1977; Hodgson *et al*. 1999).

73   Originally designed in the context of temperate herbaceous vegetation, the CSR scheme has

74   been extended to other types of vegetation (Caccianiga *et al.* 2006; Navas *et al.* 2010; Schmidtlein

75   *et al.* 2012), including a recent worldwide application (Pierce *et al.* 2017). An algorithm has

76   recently been developed to quantify the CSR scores of diverse plant species based on the

77   measurement of three leaf traits: leaf area (LA), specific leaf area (SLA) and leaf dry matter content

78   (LDMC) (Pierce *et al.* 2013, 2017). Albeit less precise than methods that consider whole-plant traits

79   which are more closely associated with stress response, competitive ability and ruderality (Hodgson

80   *et al.* 1999), classification tools based on few leaf traits have the advantage that many

81   measurements can be performed with minimal effort. This allows comparing very ecologically

82   disparate species (Pierce *et al.* 2017), or many genotypes and populations within species (May *et al.*

83   2017).

84   *Arabidopsis thaliana* is a small rosette-shaped species that is widely used in molecular

85   biology and quantitative genetics. It has recently gained a renewed interest in evolutionary ecology

86   due to the large collection of natural accessions collected from various climates and genotyped at

87   high density (Weigel 2012). Furthermore, *A. thaliana* has been shown to exhibit a significant range

88   of phenotypic variation in relation to climate, making it possible to investigate the genetic and

89   evolutionary drivers of functional diversification (Vasseur *et al*. 2018). For instance, Q_{st}-F_{st} analysis

90   has been proposed as a powerful way to discriminate adaptive and non-adaptive processes at the

91   origin of phenotypic differentiation between genetic groups, populations or lineages (Leinonen *et*

92   *al*. 2013). Indeed, this method allows one to compare the level of phenotypic differentiation (Q_{st}) to

93   the genetic differentiation (F_{st}) expected under the neutral model of population divergence. In

94   plants, this has been used to investigate the role of selection at the origin of between-populations

95   phenotypic differences related to resource-use traits (Brouillette *et al.* 2014), drought resistance

96   (Ramírez-Valiente *et al.* 2018), life history traits (Moyers and Rieseberg 2016), and functional

97   adaptation to an elevation gradient (Luo *et al.* 2015).

98   *A. thaliana* is generally described as a ruderal species that, like most annual plants,

99   reproduces quickly and invests preferentially resources to the production and dispersal of

100   propagules (Díaz *et al.* 2016; Pierce *et al.* 2017). In a recent paper, May *et al.* (2017) used the CSR

101   framework to investigate intraspecific variation in ecological strategies within this species. Using

102   16 accessions originating from contrasted climates in Europe, they found that *A. thaliana* actually

103   exhibits a wide range of variation from ruderals to stress-tolerators, with most accessions being

104   classified as intermediate (SR) and none as competitor. Interestingly, May *et al.* also found that

105   ruderality was negatively correlated with the temperature at the site where the accession originated

106   from. For instance, stress-tolerators originated predominantly from sites in hot climates (Libya,

107   Sicily and Cape Verde Islands). However, May *et al.* (2017) used a relatively low number of

108   accessions, which prevents examining the evolutionary and adaptive bases of CSR variations with

109   the environment.

110   In the present study, we analysed CSR variations on a set of 426 *A. thaliana* accessions

111   originating from contrasting climates in Europe, North Africa and East Asia. Using the

112   classification method based on three leaf traits (area, SLA and LDMC) (Pierce *et al.* 2017), we

113   tested the range of ecological strategies exhibited by these accessions. We investigated whether the

114   variation in strategies can be attributed to adaptive processes, using the genetic data available in this

115   species to perform Q_{st}-F_{st} analysis. We also examined how CSR strategies measured with leaf traits

116   correlated with whole-plant traits related to competitive ability (rosette size) and propagule

117   dispersal (fruit number). Finally, we compared our results to the findings from May *et al.* (2017),

118   and we discussed the possible causes of differences between studies such as the direction of trait-

119   environment relationships.

Materials and Methods

Plant material

122   Two experiments were performed in this study: the first one in the PHENOPSIS automaton (see

123   below) and the second one in greenhouse. In the first experiment, we used a total of 400 natural

124   accessions of *A. thaliana* L. Heynh representative of a geographical sampling from the worldwide

125   lines of the RegMap population (Horton *et al.* 2012) ($n = 214$) and from French local populations

126   (Brachi *et al.* 2013) ($n = 186$). In the second experiment, we used a total of 200 accessions from a

127   random sampling from the worldwide lines of the RegMap population. Overall, 426 accessions

128   ranging latitudinally from North Africa to Scandinavia were phenotypically characterized, 172 of

129   which were common to both experiments (Tables S1 and S2).

Experimental design

131   In Experiment 1 (PHENOPSIS), plants were grown in the high-throughput phenotyping platform

132   PHENOPSIS (Granier *et al.* 2006) in 2014, using one replicate plant per accession, except for Col-0

133   for which there were 10 replicates. Seeds were stratified in the dark at 4 °C for at least one week

134   before sowing to ensure homogeneous germination among genotypes. Four to six seeds were sown

135   at the soil surface in 225 ml pots filled with a 1:1 (v:v) mixture of loamy soil and organic compost.

136   Prior to sowing, soil surface was moistened with one-tenth strength Hoagland solution, and pots

137   were kept in the dark for 48 h under controlled environmental conditions (20 °C, 70% air relative

138   humidity). Pots were then placed in the PHENOPSIS automaton growth chamber at 20 °C, 12 h day

139   length, 70 % relative humidity, 175 µmol m^{-2} s^{-1} PPFD. Pots were sprayed with deionized water

140   three times per day until germination, soil water content was then adjusted to 0.35 g H_2O g^{-1} dry soil

141   (–0.07 MPa soil water potential) to ensure optimal growth (Aguirrezábal *et al.* 2006; Vile *et al.*

142   2012; Vasseur *et al.* 2014). After emergence of the fourth leaf, seedlings were thinned to keep only

143   one plant in each pot.

144   In Experiment 2 (Greenhouse), plants were grown in four replicates per accession in

145   greenhouse between December 2015 and May 2016. Seeds were sown on organic soil and stratified

146   at 4 °C for four days. At the emergence of the first two true leaves, plants were transplanted in 300

147   ml individual pots filled with a 1:1 (v:v) mixture of loamy soil and organic compost. Pots were

148   randomly distributed among four blocks that were rotated every day in the greenhouse. All pots

149   were watered twice a week. To reduce environmental heterogeneity in the greenhouse, walls were

150   painted in white and a semi-transparent curtain was installed below the glass roof. Additional light

151   was provided to reach *ca.* 65 µmol m^{-2} s^{-1} PPFD. Photoperiod and temperature were kept constant at

152   12 h day length, and 18/16 °C day/night, respectively.

153   **Trait measurement**

154   In both experiments, traits were measured following standardized protocols (Perez-Harguindeguy *et*

155   *al.* 2013) at a fixed phenological stage when flower buds were macroscopically visible (*i.e.* bolting

156   stage, used as measurement of flowering time, FT). The lamina of a fully-expanded, adult and non-

157   senescent leaf exposed to light was detached from the rosette, kept in deionised water at 4 °C for 24

158   h for water saturation, and then weighted (mg). After the determination of water-saturated mass,

159   individual leaves were scanned for determination of leaf lamina area (LA, mm^2) using ImageJ

160   (https://imagej.nih.gov/ij/). Dry mass of the leaf lamina was obtained after drying for 72 h at 65 °C.

161   Leaf dry matter content (LDMC, mg g^{-1}) and specific leaf area (SLA, mm^2 mg^{-1}) were calculated as

162   the ratio of lamina dry and water-saturated mass, and the ratio of lamina area to lamina dry mass,

163   respectively (Perez-Harguindeguy *et al.* 2013). In PHENOPSIS, plants were harvested at first

164   opened flower and rosette fresh mass (mg) was measured. In Greenhouse, plants were harvested

165   after full senescence and total number of fruits was manually counted on the inflorescence. Overall,

166   out of the 400 and 200 accessions in PHENOPSIS and Greenhouse, respectively 357 and 198

7

167   accessions were completely phenotyped for all traits (Tables S1 and S2), with 152 accessions

168   common to both experiments.

169   We calculated CSR scores (*i.e.* % along C, S and R axes) for all accessions in PHENOPSIS

170   and Greenhouse based on three traits: LA, LDMC and SLA, using the recent method developed by

171   Pierce *et al.* (2017). The method is based on an algorithm which combines data for three leaf traits

172   (LA, SLA and LDMC) that were shown to reliably position the position of species in the CSR

173   scheme. We calculated CSR scores for each accession using average trait value per experiment

174   using the calculation table provided in Supplementary Information of Pierce *et al.* (2017).

175   **Re-analysis of published data**

176   In our study, there were several accessions common with a previously published analysis of CSR

177   variations in *A. thaliana* (May *et al.* 2017). Ten accessions were common between May *et al.* and

178   the PHENOPSIS experiment on the one hand, and six accessions with the greenhouse experiment

179   on the other hand. In May *et al.* (2017), CSR scores were calculated based on six traits with a

180   method previously proposed by Hodgson *et al.* (1999). To compare both datasets, we first

181   recalculated CSR scores from data in May *et al.* with Pierce's method, using LA, LDMC and SLA

182   provided for their 16 accessions (May *et al.* 2017), and compared them to the CSR scores they

183   measured with the Hodgson's method.

184   **Genetic analysis and Q_{st}-F_{st} comparisons**

185   Genetic groups in *A. thaliana* were determined by clustering of 395 accessions for PHENOPSIS

186   dataset, and 198 accessions for Greenhouse dataset, both using the 250K Single Nucleotide

187   Polymorphisms (SNPs) data available from Horton *et al.* (2012). Clustering was performed with

188   ADMIXTURE (Alexander *et al.* 2009) after linkage disequilibrium pruning ($r^2 < 0.1$ in a 50 kb

189   window with a step size of 50 SNPs) with PLINK (Purcell *et al.* 2007), resulting in 24,562

190   independent SNPs. We assigned each genotype to a group if more than 60% of its genome derived

191   from the corresponding cluster. The accessions not matching this criterion were labelled

192   ''Admixed'' and were not used for the F_{st} and Q_{st} calculation. Cross-validation for different number

193 of genetic clusters revealed that the PHENOPSIS dataset was composed of six genetic groups

194 (group 1 = 74 accessions, group 2 = 48, group 3 = 18, group 4 = 55, group 5 = 5, group 6 = 71,

195 admixed = 123), while the Greenhouse dataset was composed of four genetic groups (group 1 = 38

196 accessions, group 2 = 16, group 3 = 83, group 4 = 7, admixed = 54). Consistent with the hypothesis

197 of genetic divergence because of isolation by distance, these genetic groups were geographically

198 clustered (Fig. S1). We calculated Weir and Cockerham F_{st} value for all the 24,562 SNPs, and Q_{st} as

199 the between-group phenotypic variance divided by the total phenotypic variance, using mixed-effect

200 models with Group as random factor. We used parametric bootstrap method to generate 95%

201 confidence intervals (CI) around Q_{st} values with the package '*MCMCglmm*' in R (100,000

202 iterations).

Statistical analyses

204 Genotypic means in the greenhouse experiment were estimated as the fitted genotypic values from

205 the linear models, using *lsmeans* function. Genotype effect on trait variation and broad-sense

206 heritability (H^2) were assessed using individual data from the greenhouse experiment (Table S3).

207 Genotype effect was tested with one-way ANOVA following linear modelling, using Genotype and

208 Block as explanatory variables. H^2 was measured as the ratio of phenotypic variance attributable to

209 genotypic effect over total phenotypic variance, using mixed-effect models with Block as fixed

210 factor and Genotype as random factor, using the package *nlme* in R.

211 Climate variables at the collection points of each accession were extracted from the

212 Worldclim database (http://www.worldclim.org/bioclim), with a 2.5 arc-minutes resolution. Trait-

213 trait, trait-environment and trait-CSR relationships were examined with Spearman's rank

214 coefficients of correlation (ρ), and associated *P*-values (*P*), using the function *cor.test* (Table S4).

215 Pearson's coefficients of correlations (*r*) between traits and climatic variables were also calculated

216 (Table S5). Regression lines were drawn from Standard Major Axis (SMA), using the package

217 *smatr*. All analyses were performed in R 3.2.3 (Team RC 2014).

9

Results

Trait variation and covariation

All traits varied significantly among accessions (all $P < 0.001$, Table S3). We found that FT ranged between 30 and 101 days (57 days on average) in PHENOPSIS, and between 25 to 115 days (61 days on average) in Greenhouse. Trait variation was mainly due to genetic variability among accessions, as measured by the high amount of phenotypic variance accounted for genotype effect (H^2 ranged between 0.58 for LA and 0.73 for SLA, 0.88 for FT; Table S3). Most traits were correlated with each other (Fig. S2; Tables S4,S5): SLA and LDMC were negatively correlated (Spearman's coefficient ρ = -0.94 and -0.88 in PHENOPSIS and Greenhouse, respectively, both $P <$ 0.001; Fig. S2F), and FT was positively correlated with LDMC (ρ = 0.63 and 0.86, $P < 0.001$; Fig. S2B), and negatively with SLA (ρ = -0.73 and -0.92, both $P < 0.001$; Fig. S2D).

CSR classification

A. thaliana accessions mainly varied along the S-R axis, between purely ruderals (R) to moderate stress-tolerators (S/SR) (Fig. 1). We found only three accessions (together < 1%) classified as CS, CR or CSRs. The accessions were mainly R-oriented: R, R/CR, R/CSR and R/SR represented 84% and 91% of all accessions in PHENOPSIS and Greenhouse, respectively (Table 1). Although we calculated CSR scores with only three leaf traits using the Pierce's method, whole-plant traits were consistent with our classification. For instance, the C-axis is expected to be related to plant size and height, while the R-axis is expected to be related to flowering time and seed dispersal (Grime 1977; Hodgson *et al.* 1999). Accordingly, we found that C and R-axis were positively but poorly correlated with rosette fresh mass and the total number of fruits, respectively ($\rho < 0.50$, $P < 0.05$; Fig. S3).

CSR scores were significantly correlated between PHENOPSIS and Greenhouse experiments, as measured across the 152 accessions common to both experiments (ρ = 0.34, 0.41 and 0.54 for C, S and R, respectively, all $P < 0.001$; Fig. S4). However, they were also significantly different between the two experiments ($P < 0.01$ for all the three scores). Accordingly, 78

244 accessions (51%) were classified in different CSR groups between the two experiments ("plastic"

245 accessions hereafter). Globally, plastic accessions shifted towards more ruderal strategies in

246 Greenhouse compared to PHENOPSIS, as reflected by the differences of S and R score between

247 experiments (Fig. 2). 22% of the plastic accessions were classified as R in PHENOPSIS and R/CR

248 in Greenhouse (inversely, 18% were classified as R/CR in PHENOPSIS and R in Greenhouse).

249 Comparatively, C scores did not differ a lot between the two experiments (Fig. 2B).

250 **Relationships between CSR scores, flowering time and climate**

251 Ruderality was positively correlated with SLA and mean annual temperature (MAT, °C) at the

252 collection point of the accessions, but negatively with FT and LDMC (Fig. 3; Tables S4,S5). Thus,

253 our results suggest that ruderality is typical of early-flowering plants with leaf traits representative

254 of fast resource acquisition as reflected by low LDMC and high SLA values (Wright *et al.* 2004;

255 Shipley *et al.* 2006). Inversely, stress-tolerators were characterized by late-flowering, with resource-

256 conservative trait values such as high LDMC and low SLA; which were negatively correlated with

257 MAT (Fig. S5). Consistently, S and R strategies were positively and negatively correlated with

258 latitude, respectively (Table S4).

259 Q_{st}-F_{st} analysis suggested that the latitudinal variations of CSR strategies resulted from

260 adaptive processes such as natural selection acting on leaf traits. Indeed, a value of Q_{st} significantly

261 higher than F_{st} at neutral loci is generally considered as a signature of diversifying selection on the

262 underlying traits (Leinonen *et al.* 2013). Here, we used the 95th quantile of the F_{st} distribution

263 genome-wide as a threshold of significance for phenotypic differentiation above neutral

264 expectation. In Greenhouse, both S and R scores were significantly above neutral F_{st} (Q_{st} = 0.95,

265 95% CI = [0.72-1.00], and Q_{st} = 0.82, 95% CI = [0.62-1.00] for S and R, respectively, while mean

266 F_{st} = 0.09 and F_{st} 95th quantile = 0.35; Fig. 4A). In PHENOPSIS, only R scores were above, but

267 non-significantly, neutral F_{st} (Q_{st} = 0.37 versus Fst 95th quantile = 0.33). S scores were slightly, and

268 non-significantly, below the neutral expectation (Q_{st} = 0.29, 95% CI = [0.10-0.80]; Fig. 4C). By

269 contrast, in both Greenhouse and PHENOPSIS, Q_{st} of C scores were close to 0, suggesting that this

11

270   axis of plant strategies did not vary under the influence of adaptive processes in *A. thaliana*. The

271   lower Q_{st} values reported for the PHENOPSIS experiment can be explained by the absence of

272   individual replicates in this experiment. By contrast, using genotypic mean in Greenhouse across

273   four replicates allowed reducing intra-genotypic variance, and thus total phenotypic variance

274   compared to phenotypic variance between genetic groups. Consistent with these results, plotting the

275   distribution of *A. thaliana* ecological strategies across Europe (Fig. 4B,D) revealed that accessions

276   with S-oriented strategies (S, SR, SR/CSR, S/CSR, S/SC, SC and SC/CSR) were originating from

277   northern regions, Sweden in particular.

278   **Comparison with observations from May *et al*.**

279   In contrast with our results, the 16 accessions in the study published by May *et al.* were mainly

280   categorized as S-oriented: S/SC, S/SR, S/CSR, SR and SR/CSR (Table 1, Fig. S6). May *et al.* used

281   the Hodgson's method to calculate CSR scores with seven traits, including flowering time and

282   duration, two important components of ruderality (Hodgson *et al.* 1999). To compare the two

283   classification methods, we used the traits values for LA, SLA and LDMC provided in May *et al*.

284   (2017) to calculate CSR scores with the Pierce's method and compared them with the Hodgson's

285   method. The CSR scores calculated with the two methods were positively correlated (ρ = 0.77, 0.79

286   and 0.73 for C, S and R, respectively; all *P* < 0.01; Fig. S7), suggesting that both methods return

287   similar categorization (Table 1). However and despite the significant correlations, CSR scores

288   varied substantially between the two methods (Fig. S7). This showed that the traits related to

289   ruderality (flowering time and duration) and competition (plant height and lateral spread) used in

290   the Hodgson's method impacted the inference of plant ecological strategies compared to leaf traits

291   alone.

292   FT measured in this study was strongly positively correlated with FT measured in May *et al.*

293   under controlled conditions (*n* = 10 and 6 in PHENOPSIS and Greenhouse, respectively, both *r* =

294   0.96, *P* < 0.01; Fig. S8A). By contrast, LDMC measured in May *et al.* was negatively correlated

295   with our measurements (Fig. S8D), possibly because of three individuals with early FT and

296   extremely high LDMC values (> 250 mg g^{-1}) compared to our measurement (< 110 mg g^{-1}) on the

297   same accessions (red dots in Fig. 3C). As a result, FT and LDMC were negatively, albeit non-

298   significantly, correlated in the May *et al.* study (ρ = -0.35; Fig. 3C). Furthermore, there was a

299   positive correlation between LDMC and MAT in May *et al.* ($P < 0.05$), while we found the

300   opposite in both PHENOPSIS and Greenhouse (Fig. 3B). By construction of the CSR classification

301   method, LDMC strongly participates to S and R axes (Fig. 3F and Fig. S5). Consequently, the

302   positive correlation between LDMC and MAT found in May *et al.* was associated with a positive

303   correlation between S and MAT (Fig. S5D), and inversely a negative correlation between R and

304   MAT (Fig. 3D), although these two relationships were not significant with the 16 accessions from

305   May *et al.* when using the Pierce's method of CSR classification.

Discussion

Functional adaptation to climate in *A. thaliana*

308   The relationship between CSR and climate at the interspecific level is still not well established

309   (Pierce *et al.* 2017). More broadly, trait-environment relationships remain a central question in

310   functional ecology and functional biogeography (Poorter *et al.* 2009; Violle *et al.* 2014; Borgy *et al.*

311   2017; Butler *et al.* 2017; Šímová *et al.* 2018). By contrast, adaptation to climate has been widely

312   studied within species, notably genetic adaptation along latitudinal or altitudinal gradients in annual

313   plants, and in *A. thaliana* in particular (Johanson *et al.* 2000; Picó *et al.* 2008; Banta *et al.* 2012;

314   Guo *et al.* 2012; Brachi *et al.* 2013; Wolfe and Tonsor 2014; Bloomer and Dean 2017; Tabas-

315   Madrid *et al.* 2018). Indeed, *A. thaliana* has been the model species in molecular biology, plant

316   genetics and evolution for the last decades (Bergelson and Roux 2010; Weigel 2012). It is widely

317   distributed in various climates, but is generally considered as a ruderal species that grows fast,

318   reproduces early and dies right after seed dispersal (Pierce *et al.* 2017). As expected, we found in

319   this study that *A. thaliana* was predominantly ruderal, secondly stress-tolerator and poorly

320   competitor. However, we showed an important range of CSR variation among *A. thaliana*

321   accessions along the S-R axis and associated with flowering time variation.

322   Consistent with previous studies, flowering time was positively correlated with latitude

323   (Caicedo *et al.* 2004; Lempe *et al.* 2005; Banta *et al.* 2012). For instance, northern accessions

324   exhibit late-flowering and long life cycle even when they are grown under controlled conditions in

325   growth chamber or greenhouse (Vasseur *et al.* 2018). Our results showed that flowering time was

326   positively correlated with LDMC, and that values for the two traits were higher in accessions

327   originating from higher latitude and lower temperatures. Thus, northern accessions exhibit a suite of

328   traits associated with resource conservation and longevity such as late flowering, high LDMC and

329   low SLA (Wright *et al.* 2004; Shipley *et al.* 2006; Vasseur *et al.* 2012). Q_{st}-F_{st} analysis revealed that

330   these latitudinal variations result from the adaptive diversification of leaf traits. These adaptive

331   shifts can be explained because, in cold regions, biomass production during the growing season is

332   limited by various stresses. Low temperatures directly limit plant growth rate by slowing down

333   metabolic processes. Furthermore, cold indirectly limits plant growth rate because of the reduction

334   in the availability of water and nutrients. In these conditions, slow growing genotypes with long life

335   cycle, associated with high LDMC, low SLA and low metabolic activities, can be an efficient

336   strategy. Interestingly, stress tolerance has been shown to be selected at both ends of the geographic

337   range of *A. thaliana*, but is expressed under different temperature conditions (Exposito-Alonso *et al.*

338   2018; Vasseur *et al.* 2018).

339   Conversely, ruderal strategies were more abundant in temperate and hot environments.

340   Ruderal plants are typically associated with a short life cycle, low LDMC and high SLA, and

341   presumably high metabolic rate and low tissues protection (Grime 1977). In temperate climates with

342   a relatively long growing season and high resource availability, these characteristics may allow *A.*

343   *thaliana* individuals to complete their growth cycle early and avoid competition with taller species.

344   Furthermore, in hot and dry climates with a shorter growing period (*e.g.*, Mediterranean climate),

345   fast growing strategies may allow *A. thaliana* individuals to complete their growth cycle and

346   disperse before the onset of drought, which operate as a disturbance rather than a stress, and should

347   therefore be more favourable to ruderality (Madon & Médail 1997; Volaire 2018). This result is

348 consistent with interspecific studies at global scale that reported a positive relationship between

349 SLA and temperature in herbaceous species (Borgy *et al.* 2017; Šímová *et al.* 2018). This can be

350 interpreted as a sign of selection for fast-growth, ruderal strategies in hot and stressing

351 environments at both intra- and interspecific levels (Anderegg *et al.* 2018).

352 The lack of adaptive differentiation between genetic groups along the C axis, as reflected by

353 the low Q_{st} values compared to neutral F_{st}, can be explained by the low variation of competitive

354 ability among *A. thaliana* accessions. Additionally, it could suggest that competitive environments

355 can be found in various climates as long as stress does not dominate vegetation processes. This

356 would also explain the lack of a clear geographic pattern and latitudinal gradient of competitive

357 ability across plant populations and species (Damgaard and Weiner 2017).

Influence of classification methodologies, trait measurement and growth conditions on trait-

359 **environment relationships**

360 Trait-trait, trait-CSR and trait-environment relationships were sometimes opposite between May *et*

361 *al.* (2017) and our study. For instance, May *et al.* (2017) reported a positive correlation between

362 stress-tolerance and mean temperature, while we found the opposite. A first explanation of these

363 differences is the methods used to calculate CSR scores among accessions. Although Pierce's and

364 Hodgson's scores were all positively correlated when performed on the same set of traits and

365 accessions, scores obtained from the two methods varied substantially. For instance, an accession

366 had S score at 35% with Hodgson's method but 0% with Pierce's method (Fig. S7B). The re-

367 analysis of May *et al.* data made by the authors (A. Wingler, personal communication) indicated

368 that the three accessions with very high values for S identified using the Hodgson's method (Mt-0,

369 Cvi-0 and Ct-1) were no longer in the top three ranked accessions for S when using the Pierce's

370 method, which led to a lack of correlation of S and R with temperature when using this method.

371 This can be explained because life history traits at whole-plant level, notably flowering time and

372 plant size, are important components of ruderality and competitive ability in herbaceous species

373 (Violle *et al.* 2009; Hodgson *et al.* 2017), but they are not included in the Pierce' method of CSR

400   accessions (Fig. 3C). In agreement with this hypothesis, the LDMC values measured on the early-

401   flowering accessions in our experiment were approximately half of the values estimated by May *et*

402   *al.*. As LDMC strongly participates to the S-R axis, this could explain the opposite correlations

403   between CSR and environment between the two studies. Furthermore, we found that FT was

404   positively correlated with LDMC, consistently with previous studies in a smaller set of accessions

405   (Vile *et al.* 2012), as well as in recombinant inbred lines (El-Lithy *et al.* 2010; Vasseur *et al.* 2012,

406   2014). Previous studies have notably reported that early-flowering genotypes have resource-

407   acquisitive strategies, characterized by high SLA but low LDMC and short lifespan (El-Lithy *et al.*

408   2010; Vasseur *et al.* 2012, 2014, 2018; Blonder *et al.* 2015).

409   Finally, opposite correlations between studies might also partly result from trait plasticity to

410   growth conditions. FT in *A. thaliana* is expected to vary with light conditions and temperature

411   (Mouradov *et al.* 2002). For instance, *A. thaliana* does not generally flower under short-day

412   conditions. In our study, traits were measured in controlled and constant conditions, on plants

413   grown in 12 h photoperiod and without cold exposure (*i.e.* vernalization). However, we could

414   expect FT and leaf traits, and thus CSR-environment relationships, to be different when measured

415   on plants grown outside like in May *et al.*, after vernalization or in short- or long-day conditions.

416   Consistent with this idea, we found that half the accessions common to PHENOPSIS and

417   Greenhouse did not have the same position in the CSR space: plants grown in the greenhouse were

418   generally shifted towards the R end of the spectrum compared to plants grown in PHENOPSIS.

419   This can be explained by the relative low light intensity provided by artificial lamps in the

420   greenhouse compared to the phenotyping platform (65 versus 175 µmol m^{-2} s^{-1} PPFD). In addition,

421   plants were grown in the greenhouse at higher density than in PHENOPSIS, which could have

422   increased competition for light between plants. The shade-avoidance syndrome has been described

423   as a suite of leaf trait responses to low light and competition (Kim *et al.* 2005; Mullen *et al.* 2006).

424   This includes an increase in leaf angle and SLA, associated with a reduction in LDMC and

425   flowering time (Kim *et al.* 2005; Vasseur *et al.* 2011). This is consistent with a shift towards

17

426   resource-acquisitive strategies in Greenhouse. Importantly and more broadly, controlled conditions

427   are very different from natural conditions that plants experience in the wild, and where plants

428   should ideally be measured to properly infer their ecological strategies. However, it remains

429   difficult to take into account genotype-by-environment interactions when screening genotypes in

430   natural conditions. Consequently, trait-based approaches for functional classification of plants were

431   initially proposed as a tool to infer the adaptive significance of traits in controlled conditions

432   (Grime and Hunt, 1975).

Conclusion

434   Intraspecific variation in functional strategies varied substantially along the S-R axis in *A. thaliana*.

435   Tolerance to stress seems to be favoured in cold environments at higher latitudes while ruderality is

436   predominant in temperate and hot climates. However, CSR categorization within species,

437   specifically in an herbaceous species like *A. thaliana*, is sensitive to several parameters such as the

438   type of traits used to classify accessions and the protocols used for trait measurement. Furthermore,

439   our results suggest that phenotypic plasticity to growth conditions can significantly impacts trait

440   values and thus, the determination of plant ecological strategies. This suggests that the use of trait

441   databases for local or global analyses of trait-environment relationships at species level might suffer

442   from biases due to both phenotypic plasticity and intraspecific trait variation. In a recent analysis,

443   ruderality has been demonstrated to correlate positively with the probability of naturalization of

444   alien species (Guo *et al.* 2018). In future studies, it will be interesting to examine in more details the

445   response of traits, trait combinations and strategies to environmental conditions. For instance,

446   analysing the plasticity of CSR strategies to different temperatures and water stresses could reveal

447   whether S-related strategies are constitutive or stress induced, and whether invasive species show

448   greater plasticity in ecological strategies than other species.

References

Aguirrezábal LAN, Bouchier-Combaud S, Radziejwoski A, Dauzat M, Cookson SJ, Granier C. **2006**. Plasticity to soil water deficit in *Arabidopsis thaliana*: dissection of leaf development into underlying growth dynamic and cellular variables reveals invisible phenotypes. *Plant, Cell & Environment* **29**: 2215–2227.

Albert CH, Grassein F, Schurr FM, Vieilledent G, Violle C. **2011**. When and how should intraspecific variability be considered in trait-based plant ecology? *Perspectives in Plant Ecology, Evolution and Systematics* **13**: 217–225.

Albert CH, Thuiller W, Yoccoz NG, *et al.* 2010. Intraspecific functional variability: extent, structure and sources of variation. *Journal of Ecology* **98**: 604–613.

Alexander DH, Novembre J, Lange K. 2009. Fast model-based estimation of ancestry in unrelated individuals. *Genome Research* **9**(19):1655–1664 .

Anderegg LDL, Berner LT, Badgley G, Sethi ML, Law BE, HilleRisLambers J. **2018**. Within-species patterns challenge our understanding of the leaf economics spectrum. *Ecology Letters* **21**(5): 734-744

Banta JA, Ehrenreich IM, Gerard S, *et al.* 2012. Climate envelope modelling reveals intraspecific relationships among flowering phenology, niche breadth and potential range size in *Arabidopsis thaliana*. *Ecology Letters* **15**: 769–777.

Bergelson J, Roux F. **2010**. Towards identifying genes underlying ecologically relevant traits in *Arabidopsis thaliana*. *Nature Reviews Genetics* **11**: 867–879.

Blonder B, Vasseur F, Violle C, Shipley B, Enquist BJ, Vile D. **2015**. Testing models for the leaf economics spectrum with leaf and whole-plant traits in *Arabidopsis thaliana*. *AoB plants* **7**: lv049.

Bloomer RH, Dean C. **2017**. Fine-tuning timing: natural variation informs the mechanistic basis of the switch to flowering in *Arabidopsis thaliana*. *Journal of Experimental Botany* **68**(20): 5439-5452.

Borgy B, Violle C, Choler P, *et al.* 2017. Plant community structure and nitrogen inputs modulate the climate signal on leaf traits. *Global ecology and biogeography: a journal of macroecology* **26**: 1138–1152.

Brachi B, Villoutreix R, Faure N, *et al.* 2013. Investigation of the geographical scale of adaptive phenological variation and its underlying genetics in *Arabidopsis thaliana*. *Molecular Ecology* **22**: 4222–4240.

Brouillette LC, Mason CM, Shirk RY, Donovan LA. 2014. Adaptive differentiation of traits related to resource use in a desert annual along a resource gradient. *New Phytologist* **201**(4): 1316-1327.

Butler EE, Datta A, Flores-Moreno H, *et al.* 2017. Mapping local and global variability in plant trait distributions. *Proceedings of the National Academy of Sciences of the United States of America* **114**: E10937–E10946.

Caccianiga M, Luzzaro A, Pierce S, Ceriani RM, Cerabolini B. **2006**. The functional basis of a primary succession resolved by CSR classification. *Oikos* **112**: 10–20.

Caicedo AL, Stinchcombe JR, Olsen KM, Schmitt J, Purugganan MD. **2004**. Epistatic interaction between Arabidopsis FRI and FLC flowering time genes generates a latitudinal cline in a life history trait. *Proceedings of the National Academy of Sciences of the United States of America*

491   **101**: 15670–15675.

492   **Damgaard C, Weiner J. 2017.** It's about time: a critique of macroecological inferences concerning
493   plant competition. *Trends in Ecology & Evolution* **32**(2): 86-87.

494   **Díaz S, Kattge J, Cornelissen JHC, *et al.* 2016**. The global spectrum of plant form and function.
495   *Nature* **529**: 167–171.

496   **El-Lithy ME, Reymond M, Stich B, Koornneef M, Vreugdenhil D**. **2010**. Relation among plant
497   growth, carbohydrates and flowering time in the Arabidopsis Landsberg *erecta*× Kondara
498   recombinant inbred line population. *Plant, Cell & Environment* **33**: 1369–1382.

499   **Exposito-Alonso M, Vasseur F, Ding W, Wang G, Burbano HA, Weigel D**. **2018**. Genomic
500   basis and evolutionary potential for extreme drought adaptation in *Arabidopsis thaliana*. *Nature*
501   *Ecology & Evolution* **2**: 352–358.

502   **Garnier E, Navas M-L, Grigulis K**. **2016**. *Plant Functional Diversity: Organism Traits,*
503   *Community Structure, and Ecosystem Properties*. Oxford University Press.

504   **Granier C, Aguirrezabal L, Chenu K, *et al.* 2006**. PHENOPSIS, an automated platform for
505   reproducible phenotyping of plant responses to soil water deficit in *Arabidopsis thaliana* permitted
506   the identification of an accession with low sensitivity to soil water deficit. *New Phytologist* **169**:
507   623–635.

508   **Grime JP**. **1977**. Evidence for the existence of three primary strategies in plants and its relevance to
509   ecological and evolutionary theory. *The American naturalist* **111**: 1169–1194.

510   **Grime JP, Hunt R. 1975**. Relative growth-rate: its range and adaptive significance in a local flora.
511   *Journal of Ecology* **63**(2): 393–422.

512   **Guo Y-L, Todesco M, Hagmann J, Das S, Weigel D**. **2012**. Independent FLC mutations as causes
513   of flowering-time variation in *Arabidopsis thaliana* and *Capsella rubella*. *Genetics* **192**: 729–739.

514   **Guo WY, van Kleunen M, Winter M, Weigelt P, Stein A, et al. 2018**. The role of adaptive
515   strategies in plant naturalization. *Ecology Letters* doi:10.1111/ele.13104.

516   **Hérault B, Bachelot B, Poorter L, Rossi V, Bongers F, et al. 2011**. Functional traits shape
517   ontogenetic growth trajectories of rain forest tree species. *Journal of Ecology* **99**(6): 1431-1440.

518   **Hodgson JG, Wilson PJ, Hunt R, Grime JP**. **1999**. Allocating CSR plant functional types: a soft
519   approach to a hard problem. *Oikos* 282-294.

520   **Hodgson JG, Santini BA, Montserrat Marti G *et al.* 2017**. Trade-offs between seed and leaf size
521   (seed–phytomer–leaf theory): functional glue linking regenerative with life history strategies… and
522   taxonomy with ecology? *Annals of Botany*, **120**(5): 633-652.

523   **Horton MW, Hancock AM, Huang YS, *et al.* 2012**. Genome-wide patterns of genetic variation in
524   worldwide Arabidopsis thaliana accessions from the RegMap panel. *Nature Genetics* **44**: 212–216.

525   **Johanson U, West J, Lister C, Michaels S, Amasino R, Dean C**. **2000**. Molecular analysis of
526   FRIGIDA, a major determinant of natural variation in Arabidopsis flowering time. *Science* **290**:
527   344–347.

528   **Keddy PA. 1992**. A pragmatic approach to functional ecology. *Functional Ecology* **6**(6): 621–626.

Kim GT, Yano S, Kozuka T, Tsukaya H. **2005**. Photomorphogenesis of leaves: shade-avoidance and differentiation of sun and shade leaves. *Photochemical & photobiological sciences: Official journal of the European Photochemistry Association and the European Society for Photobiology* **4**: 770–774.

Leinonen T, McCairns RS, O'hara R B, Merilä J. 2013. Q_{ST}–F_{ST} comparisons: evolutionary and ecological insights from genomic heterogeneity. *Nature Reviews Genetics* **14**(3): 179.

Lempe J, Balasubramanian S, Sureshkumar S, Singh A, Schmid M, Weigel D. **2005**. Diversity of flowering responses in wild *Arabidopsis thaliana* strains. *PLoS Genetics* **1**: 109–118.

Luo Y, Widmer A, Karrenberg S. 2015. The roles of genetic drift and natural selection in quantitative trait divergence along an altitudinal gradient in *Arabidopsis thaliana*. *Heredity* **114**(2): 220.

Madon O, Médail F. 1997. The ecological significance of annuals on a Mediterranean grassland (Mt Ventoux, France). *Plant Ecology* **129**(2): 189-199.

May R-L, Warner S, Wingler A. **2017**. Classification of intra-specific variation in plant functional strategies reveals adaptation to climate. *Annals of Botany* **119**: 1343–1352.

Mouradov A, Cremer F, Coupland G. **2002**. Control of flowering time. *Plant Cell* **14**: S111–S130.

Moyers BT, Rieseberg LH. 2016. Remarkable life history polymorphism may be evolving under divergent selection in the silverleaf sunflower. *Molecular Ecology* **25**(16): 3817-3830.

Mullen JL, Weinig C, Hangarter RP. **2006**. Shade avoidance and the regulation of leaf inclination in Arabidopsis. *Plant, Cell & Environment* **29**: 1099–1106.

Navas M-L, Roumet C, Bellmann A, Laurent G, Garnier E. **2010**. Suites of plant traits in species from different stages of a Mediterranean secondary succession. *Plant Biology* **12**: 183–196.

Perez-Harguindeguy N, Diaz S, Garnier E, *et al*. 2013. New handbook for standardised measurement of plant functional traits worldwide. *Australian Journal of Botany* **61**(3): 167-234.

Picó FX, Méndez-Vigo B, Martínez-Zapater JM, Alonso-Blanco C. **2008**. Natural genetic variation of Arabidopsis thaliana is geographically structured in the Iberian peninsula. *Genetics* **180**: 1009–1021.

Pantin F, Simonneau T, Muller B. 2012. Coming of leaf age: control of growth by hydraulics and metabolics during leaf ontogeny. *New Phytologist* **196**(2): 349-366.

Pierce S, Brusa G, Vagge I, Cerabolini BEL. **2013**. Allocating CSR plant functional types: the use of leaf economics and size traits to classify woody and herbaceous vascular plants. *Functional Ecology* **27**: 1002–1010.

Pierce S, Negreiros D, Cerabolini BEL, *et al.* 2017. A global method for calculating plant CSR ecological strategies applied across biomes world-wide. *Functional ecology* **31**: 444–457.

Poorter H, Niinemets Ü, Poorter L, Wright IJ, Villar R. **2009**. Causes and consequences of variation in leaf mass per area (LMA): a meta-analysis. *New Phytologist* **182**: 565–588.

Purcell S, Neale B, Todd-Brown K, Thomas L, Ferreira MA, et al. 2007. PLINK: a tool set for whole-genome association and population-based linkage analyses. *The American Journal of Human*

21

568   *Genetics* **81**(3): 559-575.

569   **Ramírez‑Valiente JA, Deacon NJ, Etterson J, Center A, Sparks JP, Sparks KL, Longwell T,**
570   **Pilz G, Cavender‑Bares J. 2018.** Natural selection and neutral evolutionary processes contribute to
571   genetic divergence in leaf traits across a precipitation gradient in the tropical oak *Quercus oleoides*.
572   *Molecular Ecology* **27**(9): 2176-2192.

573   **Reich PB, Ellsworth DS, Walters MB,** *et al.* **1999**. Generality of leaf trait relationships : A test
574   across six biomes. *Ecology* **80**: 1955–1969.

575   **Schmidtlein S, Feilhauer H, Bruelheide H**. **2012**. Mapping plant strategy types using remote
576   sensing. *Journal of vegetation science: official organ of the International Association for*
577   *Vegetation Science* **23**: 395–405.

578   **Shipley B, Lechowicz MJ, Wright I, Reich PB**. **2006**. Fundamental trade-offs generating the
579   worldwide leaf economics spectrum. *Ecology* **87**: 535–541.

580   **Siefert A, Violle C, Chalmandrier L,** *et al.* **2015**. A global meta-analysis of the relative extent of
581   intraspecific trait variation in plant communities. *Ecology Letters* **18**: 1406–1419.

582   **Šímová I, Violle C, Svenning J-C,** *et al.* **2018**. Spatial patterns and climate relationships of major
583   plant traits in the New World differ between woody and herbaceous species. *Journal of*
584   *Biogeography* **45**(4): 895-916.

585   **Tabas-Madrid D, Méndez-Vigo B, Arteaga N,** *et al.* **2018**. Genome-wide signatures of flowering
586   adaptation to climate temperature: regional analyses in a highly diverse native range of *Arabidopsis*
587   *thaliana*. *Plant, Cell & Environment* 1-15.

588   **Team RC**. **2014**. R: A language and environment for statistical computing. R Foundation for
589   Statistical Computing, Vienna, Austria. 2013.

590   **Vasseur F, Bontpart T, Dauzat M, Granier C, Vile D**. **2014**. Multivariate genetic analysis of
591   plant responses to water deficit and high temperature revealed contrasting adaptive strategies.
592   *Journal of Experimental Botany* **65**: 6457–6469.

593   **Vasseur F, Exposito-Alonso M, Ayala-Garay OJ,** *et al.* **2018**. Adaptive diversification of growth
594   allometry in the plant *Arabidopsis thaliana*. *Proceedings of the National Academy of Sciences of the*
595   *United States of America*: 201709141.

596   **Vasseur F, Pantin F, Vile D**. **2011**. Changes in light intensity reveal a major role for carbon
597   balance in Arabidopsis responses to high temperature. *Plant, Cell & Environment* **34**: 1563–1579.

598   **Vasseur F, Violle C, Enquist BJ, Granier C, Vile D**. **2012**. A common genetic basis to the origin
599   of the leaf economics spectrum and metabolic scaling allometry. *Ecology Letters* **15**: 1149–1157.

600   **Vile D, Pervent M, Belluau M,** *et al.* **2012**. Arabidopsis growth under prolonged high temperature
601   and water deficit: independent or interactive effects? *Plant, Cell & Environment* **35**: 702–718.

602   **Violle C, Enquist BJ, McGill BJ,** *et al.* **2012**. The return of the variance: intraspecific variability in
603   community ecology. *Trends in Ecology & Evolution* **27**: 244–252.

604   **Violle C, Garnier E, Lecoeur J, Roumet C, Podeur C, Blanchard A, Navas ML 2009.**
605   Competition, traits and resource depletion in plant communities. *Oecologia* **160**(4): 747-755.

606   **Violle C, Navas ML, Vile D,** *et al.* **2007**. Let the concept of trait be functional! *Oikos* **116**: 882–

607   892.

608   **Violle C, Reich PB, Pacala SW, Enquist BJ, Kattge J. 2014.** The emergence and promise of
609   functional biogeography. *Proceedings of the National Academy of Sciences of the United States of*
610   *America*, **111**(38): 13690-13696.

611   **Volaire F**. **2018**. A unified framework of plant adaptive strategies to drought: crossing scales and
612   disciplines. *Global Change Biology* **24**(7): 2929-2938.

613   **Walters MB, Kruger EL, Reich PB. 1993.** Relative growth rate in relation to physiological and
614   morphological traits for northern hardwood tree seedlings: species, light environment and
615   ontogenetic considerations. *Oecologia* **96**(2): 219-231.

616   **Weigel D**. **2012**. Natural variation in Arabidopsis: from molecular genetics to ecological genomics.
617   *Plant Physiology* **158**: 2–22.

618   **Wolfe MD, Tonsor SJ**. **2014**. Adaptation to spring heat and drought in northeastern Spanish
619   *Arabidopsis thaliana*. *New Phytologist* **201**: 323–334.

620   **Wright IJ, Reich PB, Westoby M,** *et al.* **2004**. The worldwide leaf economics spectrum. *Nature*
621   **428**: 821–827.

Figure legends

Figure 1. CSR variation in *A. thaliana*. (**A**) CSR representation of the 357 accessions from PHENOPSIS. (**B**) CSR representation of the 198 accessions from Greenhouse. Dots are coloured by CSR scores, following colour code provided in Pierce *et al.* (2017).

Figure 2. Plasticity of CSR classification in *A. thaliana*. (**A**) The 78 plastic accessions that have different CSR classification between PHENOPSIS and Greenhouse experiments are plotted. Arrows start at Greenhouse position and end at PHENOPSIS position, they are coloured according to CSR scores in PHENOPSIS, following colour code provided in Pierce *et al.* (2017). (**B**) Boxplot representing the difference in CSR scores between experiments (Greenhouse values – PHENOPSIS values).

Figure 3. Relationships between ruderality, traits and environment in *A. thaliana*. Leaf trait and flowering time data were obtained from May *et al*. (2017) (red dots, $n = 16$), PHENOPSIS (green dots, $n = 357$) and Greenhouse (blue dots, $n = 198$). Ruderality (R) was calculated with Pierce's method (2017) for all data. Mean annual temperature (MAT, °C) was extracted at the collection point of the accessions with Worldclim. FT: flowering time (days), LDMC: leaf dry matter content (mg g^{-1}). ρ represents Spearman's coefficient of correlation. Significance code: ^{NS}: $P > 0.1$, ˙: $P < 0.1$, *: $P < 0.05$, **: $P < 0.01$,***; $P < 0.001$. Regression lines were drawn from standard major axis (SMA).

Figure 4. Q_{st}-F_{st} analysis and geographic location of CSR strategies in *A. thaliana*. Distribution (in grey) of F_{st} values across the 24,562 SNPs with 95th quantile threshold of non-neutral expectation (dashed line), and Q_{st} values for the C, S and R scores measured as the ratio of phenotypic variance between genetic groups over total phenotypic variance. Analysis performed independently on Greenhouse dataset (**A**), and PHENOPSIS dataset (**C**). Geographic location of CSR strategies with Greenhouse dataset (**B**, $n = 198$), and PHENOPSIS dataset (**D**, $n = 357$).

24

Table 1. Proportion (%) of ecological strategies among *A. thaliana* accessions.

	PHENOPSIS	*Greenhouse*	*Original scores from May et al.*	*Recalculated scores with data from May et al. 2017*
R	25.5	24.2		31.3
R/CR	47.6	58.6	12.5	
R/CSR	8.7	7.1		
R/SR	2.2	1.5	6.2	6.2
SR/CSR	8.4	4.5		12.5
SR	0.6	3.5	56.3	25.0
S	0.2			
S/CSR	3.1	0.6		18.7
S/SC			25.0	
S/SR	2.8			6.3
CSR	0.3			
CS	0.3			
CR	0.3			

List of Supplementary Information

Table S1. Phenotypic traits measured in PHENOPSIS experiment.

Table S2. Phenotypic traits measured in Greenhouse experiment.

Table S3. Heritability and genetic effects on traits measured in Greenhouse experiment.

Table S4. Spearman's pairwise correlations between traits and environments.

Table S5. Pearson's pairwise correlations between traits and environments.

Figure S1. Geographic location of the genetic groups defined with SNPs clustering. (**A**) Representation of the six genetic groups (+ admixed) identified in the PHENOPSIS dataset ($n = 394$). (**B**) Representation of the four genetic groups (+ admixed) identified in the Greenhouse dataset ($n = 198$).

25

669   **Figure S2. Trait-trait relationships in *A. thaliana*.** PHENOPSIS (blue dots, $n = 357$) and

670   Greenhouse (green dots, $n = 198$). ρ represents Spearman's coefficient of correlation. Significance

671   code: NS: $P > 0.1$, ∵: $P < 0.1$, *: $P < 0.05$, **: $P < 0.01$,***; $P < 0.001$. Regression lines were drawn

672   from standard major axis (SMA).

673   **Figure S3. Correlations between C and R axes, plant biomass and fruit number.** (**A**)

674   Correlation between C axis and rosette fresh weight (mg) measured in PHENOPSIS (blue dots, $n =$

675   357). (**B**) Correlation between R axis and fruit number measured in Greenhouse (green dots, $n =$

676   198). ρ represents Spearman's coefficient of correlation. Significance code: NS: $P > 0.1$, ∵: $P < 0.1$,

677   *: $P < 0.05$, **: $P < 0.01$,***; $P < 0.001$. Regression lines were drawn from standard major axis

678   (SMA).

679   **Figure S4. Correlations between CSR scores in PHENOPSIS and Greenhouse experiments.**

680   Correlations were estimated on the set of 152 accessions common to both experiments. ρ represents

681   Spearman's coefficient of correlation. Significance code: NS: $P > 0.1$, ∵: $P < 0.1$, *: $P < 0.05$, **: $P <$

682   0.01,***; $P < 0.001$. Regression lines were drawn from standard major axis (SMA).

683   **Figure S5. CSR-traits and CSR-environment relationships in *A. thaliana*.** Leaf trait and

684   flowering time data were obtained from May *et al*. (2017) (red dots, $n = 16$), PHENOPSIS (blue

685   dots, $n = 357$) and Greenhouse (green dots, $n = 198$). Ruderality (R), stress-tolerance (S), and

686   competitive ability (C) were calculated with Pierce's method (2017) for all data. Mean annual

687   temperature (MAT, °C) was extracted at the collection point of the accessions with Worldclim. FT:

688   flowering time (days), LDMC: leaf dry matter content (mg g^{-1}). ρ represents Spearman's coefficient

689   of correlation. Significance code: NS: $P > 0.1$, ∵: $P < 0.1$, *: $P < 0.05$, **: $P < 0.01$,***; $P < 0.001$.

690   Regression lines were drawn from standard major axis (SMA).

691   **Figure S6. CSR representation of the 16 accessions from May *et al.* (2017).** CSR scores

692   recalculated with leaf trait data using Pierce's (2017) method. Dots are coloured by CSR scores,

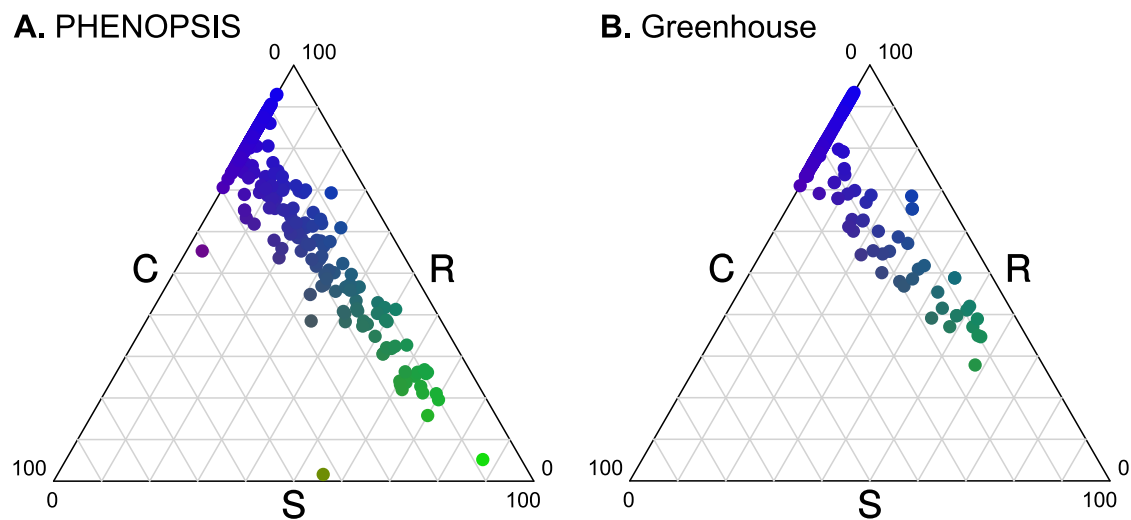693   following colour code provided in Pierce *et al.* (2017).

694   **Figure S7. Correlation between Hodgson's and Pierce's methods for quantifying CSR.** CSR

695   scores were recalculated with leaf traits provided for the 16 accessions in May *et al.* (2017), using

696   Pierce's method, and compared to CSR scores measured in May *et al.* (2017) with Hodgson's

697   method. ρ represents Spearman's coefficient of correlation. Significance code: [NS]: $P > 0.1$, ˙: $P <$

698   0.1, *: $P < 0.05$, **: $P < 0.01$,***; $P < 0.001$. Regression lines were drawn from standard major axis
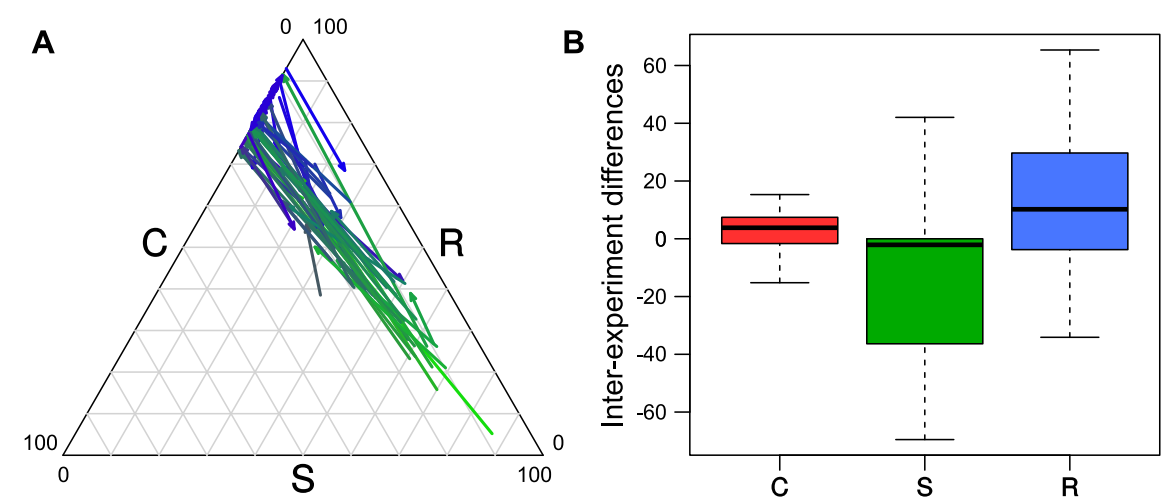
699   (SMA).

700   **Figure S8. Correlations between traits measured in May *et al.* and the present study.**

701   Correlations were estimated on the 10 and 6 accessions common to May *et al.* (2017) and

702   PHENOPSIS (blue dots) and Greenhouse (green dots) experiments, respectively. ρ represents

703   Spearman's coefficient of correlation. Significance code: [NS]: $P > 0.1$, ˙: $P < 0.1$, *: $P < 0.05$, **: $P <$

704   0.01,***; $P < 0.001$. Regression lines were drawn from standard major axis (SMA). FT: flowering

705   time (days), LA: leaf area (mm^2), LDMC: leaf dry matter content ($mg\ g^{-1}$), SLA: specific leaf area
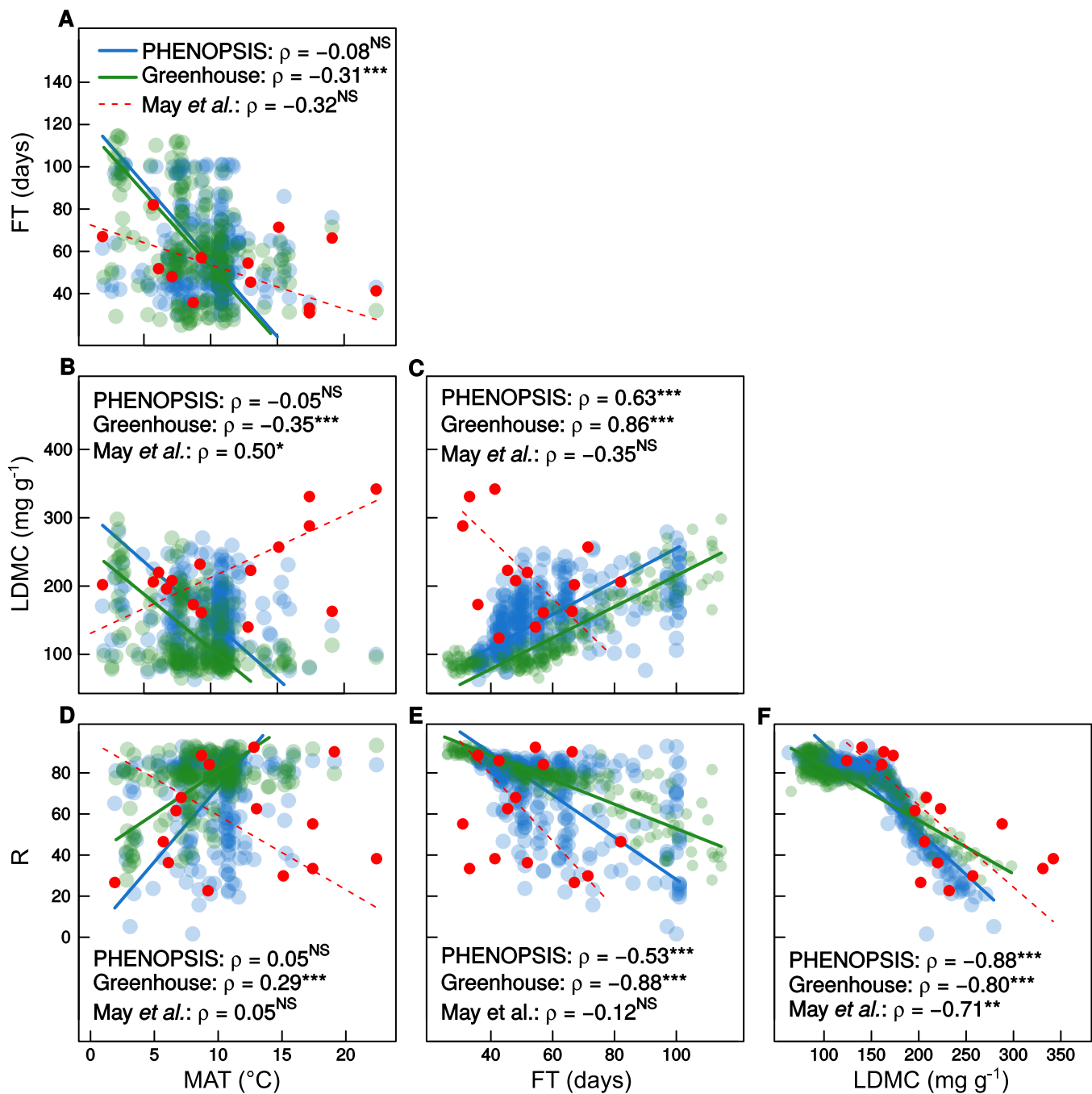
706   ($m^2\ kg^{-1}$).

Figure 1.

A. PHENOPSIS

B. Greenhouse

Figure 2.

Figure 3.

Figure 4.